eprints@whiterose.ac.uk
https://eprints.whiterose.ac.uk/

ARTICLE TYPE

A ratiometric sensor for DNA based on a dual emission Ru(dppz) light-switch complex

Michael G. Walker,[a] Vadde Ramu,[b] Anthony J. H. M. Meijer,[a]* Amitava Das,[b,c]* and Jim A Thomas[a]*

Herein we describe the DNA binding properties of two new water-soluble ruthenium complexes; experimental and computational data reveal that both complexes display dual emission from MLCT and LLCT excited states. The interaction of the new complexes with DNA was also investigated. Although one of the complex only binds DNA though groove binding, the second complex has seperate ligands
10 capable of groove binding and intercalation. Nevertheless, it was found that both complexes interact with duplex DNA with high affinity. DNA induced distinctive changes in the emission of the complexes; although the groove binding complex only displays a modest increase in emission on binding, the complex that contains the intercalating Ru^{II}(dppz) moiety displays a large increase in MLCT-based emission on DNA binding while emission from LLCT excited state is unaffected. This means that the
15 complex functions as the first ratiometric sensor for DNA.

Introduction

Since the discovery that $[Ru(N-N)_2(dppz)]^{2+}$ (where dppz = dipyridylphenazine and N-N = 2,2'-bipyridyl, 1,10-phenanthroline) displays a "DNA light-switch" effect, in which
20 its triplet based, metal-to-ligand charge-transfer ^{3}MLCT-based emission is "switched on" through intercalation,[1] a huge number of studies have been carried out on this complex and its derivatives. These systems have potential application as general optical probes for DNA,[2-7] and can also be used to detect specific
25 structures, for example mismatches.[8,9] The original complex, and a closely related Re^I derivative, have also been employed as switch-on optical probes to monitor the aggregation of amyloidogenic proteins such as amyloid-β and α-synuclein.[10-13]

However, whilst such off-on responses can be exploited in
30 sensing, luminescence-based ratiometric probes[14-17] are more convenient as their response is independent of probe concentration. This facilitates accurate and quantitative determination of analyte concentrations *irrespective* of probe concentrations. Unsurprisingly, ratiometric sensors are much
35 sought after, and have been developed for a wide range of analytes[18-22]. Despite these advantages, a convenient ratiometric sensor for DNA is yet to be developed.

As part of a program to synthesize novel DNA binding systems,[23-30] the Thomas group has investigated the properties of
40 achiral $[Ru(tpm)(L)(dppz)]^{2+}$ complexes (where tpm = tris(pyrazolyl)methane, L = a monodentate N-donor ligand) as building blocks for the construction of mixed motif[31-34] and oligonuclear[35,36] DNA recognition systems. This work has revealed that even small changes in ancillary ligand structure can
45 have profound effects on the photophysical and biophysical properties of these metallo-intercalators.[32,37] Together, the

Thomas and Das groups recently reported on extended Ru^{II} complexes that groove bind to duplex DNA with high affinity and good sequence selectivity.[38] Herein, we report that a system
50 incorporating features from both these series of complexes is the first small molecule ratiometric sensor for DNA.

Although it is usually assumed that emission is solely from the lowest photo-excited state - due to their wide range of potential excited states - reports on d^6-metal complexes displaying dual
55 emission are now relatively common.[39-45] In this case, since other $[Ru(tpm)(L)(dppz)]^{2+}$ complexes do not show this effect, it seems that incorporation of DMSP (where DMSP = (E)-4-(3,4-dimethoxystyryl)pyridine) is associated with dual emission. Experimental and computational studies on the optical properties
60 of 1^{2+} and 2^{2+} in comparison with $[Ru(tpm)(py)(dppz)]^{2+}$ provides further evidence for this conclusion.

Experimental

Synthesis

[**1**](PF$_6$)$_2$ Ru(tpm)(dppz)Cl]Cl (0.1g, 0.15 mmol) and AgNO$_3$ (2.2
65 eq, 55.9 mg, 0.33 mmol) were refluxed in 40 cm³ ethanol-water [3:1] for 5 hours in the absence of light. After cooling to room temperature the solution was filtered through celite to remove the precipitated AgCl as a white powder. Excess DMSP (10 eq, 0.36 g, 1.49 mmol) was added to the filtrate and the solution refluxed
70 overnight. The volume was reduced to dryness and the resulting solid re-dissolved in water. Aqueous NH$_4$PF$_6$ (10 eq, 0.24 g, 1.50 mmol) was added to the solution, which was refrigerated, resulting in precipitation of the complex. The crude orange product was collected by filtration and washed with water and
75 diethyl ether before being dried under vacuum. The resulting PF$_6$ salt was dissolved in acetone and tetrabutylammonium chloride

(10 eq, 0.42 g, 1.50 mmol) dissolved in acetone was added. The resulting solution was refrigerated overnight and the volume reduced to dryness. The crude chloride product was dissolved in acetonitrile and purified over neutral alumina using acetonitrile/water [98:2, v/v] as eluent. The major band was collected, yielding the pure chloride form of the compound. The product was converted to the corresponding PF_6 salt for characterization purposes. Mass (Yield) = 71.2 mg (57%).

^{1}H NMR (400 MHz, CD$_3$CN): δ_H = 9.82 (dd, J = 8.2, 1.2 Hz, 2H), 9.15 (s, 1H), 9.11 (dd, J = 5.4, 1.2 Hz, 2H),8.63 (d, J = 2.8 Hz, 2H), 8.59 (dd, J = 6.6, 3.4 Hz, 2H), 8.39 (d, J = 2.8 Hz, 1H), 8.23 (dd, J = 6.5, 3.4 Hz, 2H),8.14 (d, J = 2.1 Hz, 2H), 8.06 (dd, J = 8.2, 5.4 Hz, 2H), 7.32 (d, J = 6.8 Hz, 2H), 7.32 (d, J = 16.3 Hz, 1H), 7.15(d, J = 1.8 Hz, 1H), 7.11 (d, J = 6.8 Hz, 2H), 7.07 (dd, J = 8.4, 1.8 Hz, 1H), 6.94 (d, J = 15.6 Hz, 1H), 6.91 (d, J = 8.2 Hz, 1H), 6.86 { 6.84 (m, 2H), 6.47 (d, J = 2.2 Hz, 1H), 6.21 { 6.20 (m, 1H), 3.81 (s, 6H). Elemental analysis: Calculated for C$_{43}$H$_{35}$F$_{12}$N$_{11}$O$_2$P$_2$Ru.3H$_2$O: Carbon (Expected value: 43.33%): Found: 42.93% Hydrogen (Expected value: 3.53%): Found: 3.03% Nitrogen (Expected value: 12.93%): Found: 12.55%.ES-MS, m/z (%): 419. [M-2PF$_6$]$^{2+}$, 838 [M-2PF$_6$-H]$^+$, 984 [M-PF$_6$]$^+$. Accurate Mass MS for m/z = 838 peak: Formula: C$_{43}$H$_{34}$N$_{11}$O$_2$Ru Theoretical m/z = 838.1940. Found = 838.1999.

[**2**](PF$_6$)$_2$ [Ru(tpm)(phen)Cl]Cl (0.1g, 0.18 mmol) and AgNO$_3$ (2.2 eq, 66.0 mg, 0.39 mmol) were refluxed in 40 cm3 ethanol-water [3:1] for 5 hours in the absence of light. After cooling to room temperature the solution was filtered through celite to remove the precipitated AgCl as a white powder. Excess DMSP (10 eq, 0.43 g, 1.77 mmol) was added to the filtrate and the solution refluxed overnight in darkness. The volume was reduced to dryness and the resulting solid re-dissolved in water. Aqueous NH$_4$PF$_6$ (10 eq, 0.29 g, 1.77 mmol) was added to the solution, which was refrigerated, resulting in precipitation of the complex. The crude orange product was collected by filtration and washed with water and diethyl ether before being dried under vacuum. This solid was dissolved in acetone and an acetone solution of tetrabutylammonium chloride (10 eq, 0.49 g, 1.77 mmol) was added. The resulting solution was refrigerated overnight and the volume reduced to dryness. The crude chloride product was dissolved in acetonitrile and purified through chromatography over neutral alumina using acetonitrile/water [98:2, v/v] as eluent. The major band was collected, and the required hexafluorophospate salt was isolated through the addition of NH$_4$PF$_6$. The resultant precipitate was collected by filtration and washed with water and diethyl ether before being dried under vacuum.
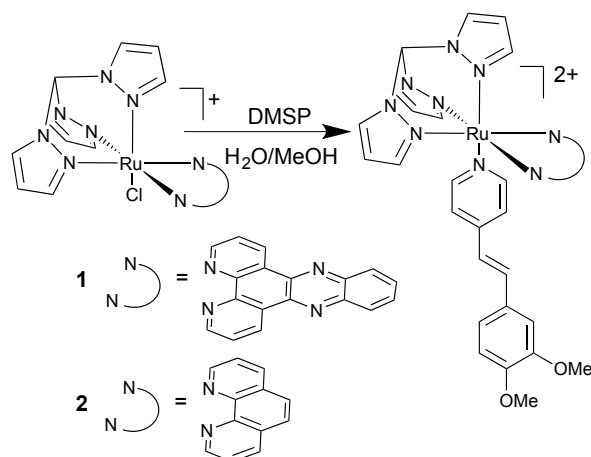
1H NMR (400 MHz, CD$_3$CN): δ_H = 9.10 (s, 1H), 9.03 (dd, J = 5.2, 1.1 Hz, 2H), 8.78 (dd, J = 8.2, 1.1 Hz, 2H), 8.60 (d, J = 2.8 Hz, 2H), 8.44 (s, 2H), 8.34 (d, J = 2.9 Hz, 1H), 8.11 (d, J = 2.1 Hz, 2H), 7.91 (dd, J = 8.2, 5.3 Hz, 2H), 7.31 (d, J = 16.3 Hz, 1H), 7.16 (d, J = 1.9 Hz, 1H), 7.15 – 7.12 (m, 2H), 7.09 – 7.05 (m, 3H), 6.93 (d, J = 16.2 Hz, 1H), 6.93 (d, J = 8.5 Hz, 1H), 6.84 – 6.81 (m, 2H), 6.15 – 6.12 (m, 1H), 6.03 (d, J = 2.2 Hz, 1H), 3.83 (s, 3H), 3.82 (s, 3H). ES-MS, m/z (%):369 [M-2PF$_6$]$^{2+}$, 736 [M-2PF$_6$]+, 882 [M-PF$_6$]+. Elemental analysis: Molecular formula: C$_{37}$H$_{33}$F$_{12}$N$_9$O$_2$P$_2$Ru: Carbon (Expected value: 43.28%): Found: 42.72% Hydrogen (Expected value: 3.24%): Found: 3.21% Nitrogen (Expected value: 12.28%): Found: 11.90%.

Computational methods

See supplementary information for details

Results and Discussion

Since our previous study on Ru^{II} complexes involved using the bidentate (E)-4-[2-(4'-methyl-2,2'-bipyridin-4-yl)vinyl]benzene-1,2-diol as the groove-binding ligand, we sought to invesigate a related structure, DMSP, that could be coordinated to the Ru^{II}(tpm) moiety in a monodentate manner. The DMSP ligand was prepared by an established method,[46,47] and then coordinated to Ru^{II}(tpm)-based starting materials to yield complexes **1**$^{2+}$ and **2**$^{2+}$ as hexafluorophosphate salts – Scheme 1.

Scheme 1 Synthesis of complexes **1** and **2**.

Although standard spectroscopic methods indicated the complexes were analytically pure after the outlined syntheses, samples of the complexes used for optical and biological studies were further purified by reverse phase HPLC on a Agilent 1260 Infinity system eluted with acetonitrile/water solvent mixture.

Optical studies

The absorbance spectra of the complexes in MeCN (See Fig S2 and S3) are summarized in Table 1.

Table 1 Summary of optical data for **1**$^{2+}$ and **2**$^{2+}$.[a]

Complex	Absorbance λ_{max}/nm ($10^{-3}\varepsilon$/M^{-1}cm^{-1})	Emission[b] λ_{em}/nm
1^{2+}	204 (69.5), 230 (sh), 277 (66.1), 318 (sh), 362 (32.1), 391 (28.9), 425 (sh), 500 (sh)	540, 626
2^{2+}	203 (74.5), 226 (sh), 267 (53.6), 289 (sh), 313 (15.5), 358sh, 390 (28.5), 425 (sh), 470 (sh)	540, 671

[a] Reported for hexafluorophosphate salts in MeCN. [b]λ_{ex} = 425 nm

The high-energy transitions are dominated by ligand-based $\pi \rightarrow \pi^*$ transitions. For example, both complexes possess an intense band at 203 nm with a shoulder at 230 nm (for **1**$^{2+}$) and 226 nm (for **2**$^{2+}$). In MeCN the free DMSP ligand displays an intense band centred at 200 nm, whereas the free tpm ligand shows a

single peak at 219 nm with an excitation coefficient of around half that of the DMSP band. Therefore the high energy band and shoulder in 1^{2+} and 2^{2+} are assigned to the $\pi \rightarrow \pi^*$ transitions of the coordinated DMSP and tpm ligands respectively. Bands between 250 – 350 nm can be assigned to similar $\pi \rightarrow \pi^*$ transitions in the coordinated polypyridyl ligands. At lower energies both complexes also display broad, less intense, bands with shoulders that stretch out beyond 500 nm; these transitions are assigned to charge transfer processes, *vide infra*.
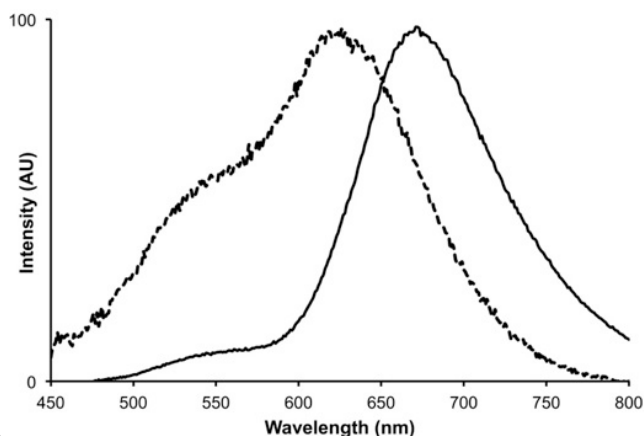

Fig. 1 Emission spectra of 1^{2+} (solid line) and 2^{2+} (broken line) recorded in acetonitrile. (λ_{ex} = 425 nm). NB.; normalized for comparative purposes

The emission data for both complexes is also summarized in Table 1. In acetonitrile, excitation into the ^{1}MLCT band produces low energy emissions, at 626 nm and 671 nm for 1^{2+} and 2^{2+} respectively, characteristic of ^{3}MLCT-based emission. However, both complexes also display a distinctive high-energy shoulder at 540 nm. Due to the more intense ^{3}MLCT-based emission of 1^{2+} this shoulder is relatively less prominent than for 2^{2+}, but it is still clearly visible in the normalized spectra shown in Fig 2. The intensity ratio of the shoulder and the lower energy main band remain invariant, even after meticulous purification of both complexes confirms that it not an impurity. Furthermore, these emissions come at energies that are entirely different to the free ligand – Fig 2A. Furthermore, and crucially, analysis of the excitation spectrum of each emission shows they are due to the complexes and not DMSP or another impurity – Fig 2B.
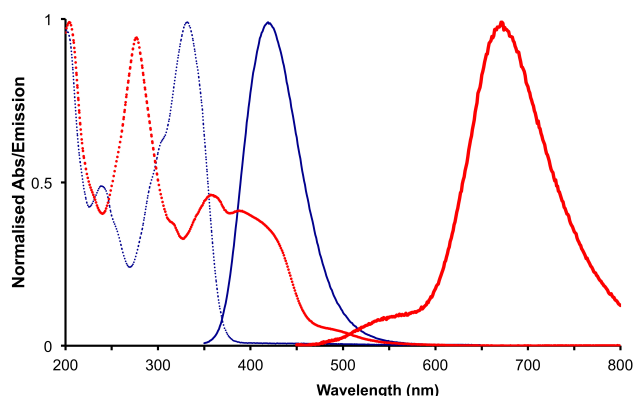

Fig. 2 A comparison of the absorption (broken lines) and emission (bold lines) spectra of free DMSP ligand (blue) and complex [**1**](PF$_6$)$_2$ (red) in air equilibrated HPLC (extra pure) grade acetonitrile.

Quantum yield (ϕ) measurements for complex 1^{2+} at the two different wavelengths were found to be $\phi_{(550)}$ = 9.7 x 10^{-4} and $\phi_{(671)}$ = 3.6 x 10^{-3}, respectively. The value for the longer wavelength is very close to that reported for [Ru(tpm)(py)(dppz)]$^{2+}$ (py = pyridine, ϕ = 2.0 x 10^{-3}).[34] Time correlated single photon counting studies were also carried out with 1^{2+} in air equilibrated acetonitrile medium using 406 nm laser as an excitation source.

Time resolved emission decay traces monitored at 550 nm (λ_{Ext} = 406 nm) are best fitted to a short lived excited state exhibiting biexponential decay with τ_{Avg} = 0.35 ns (τ_1 = 0.17 ns (59%) and τ_2 = 0.61 ns (41%). Similar studies monitored at 680 nm yielded decay traces that could also be fitted to a biexponential decay constants of τ_1 = 0.4 ns (59%) and τ_2 = 48.2 ns (39%). (See SI, Fig S4 and S5) Previous studies on [Ru(tpm)(py)(dppz)]$^{2+}$ have revealed a lifetime of ~75 ns in deaerated acetonitrile solution for the Ru$_{d\pi} \rightarrow$ dppz$_{\pi^*}$ based ^{3}MLCT excited states.[34] Thus, the time constant of = 48.2 ns (τ_2) observed in the aerated solution is attributed to the expected Ru$_{d\pi} \rightarrow$ dppz$_{\pi^*}$ based ^{3}MLCT excited state, while the shorter component (τ_1 = 0.4 ns) is due to equilibration with the high energy 550 nm emission excited state.

As mentioned above, the number of metal complexes that break Kasha's rule by displaying dual emission has burgeoned.[39-45,48,49] In these cases, the second emission is often assigned to a ligand-based intramolecular charge transfer, ICT[50] or a ligand-to-ligand charge transfer, LLCT.[42,51] Indeed, a stimulating recent review has suggested that dual or even multiple emission from ^{3}MLCT states of Ru^{II} complexes is not extraordinary and postulates that specific ion pairing interactions result in excited state electron densities that are localized on individual ligands - or even sections of ligands - to produce several MLCT emission states.[52] Certainly, the observations of multiple lifetimes in the time resolved studies on 1^{2+} are suggestive of this latter possibility. It should be noted that, although the free DMSP ligand does display an ICT,[47] this is at 420 nm in acetonitrile Fig. 2. The possibility that Ru^{II} coordination could lower the energy of the ICT to produce the emission at 550 nm, was discounted through density functional theory, DFT, calculations on both complexes and the free DMSP ligand. Further DFT studies provided greater insights into the possible emissive states of complex 2^{2+}.

Computational studies

The optimized structures for the S$_0$ ground state for DMSP and its S$_1$ excited state are given in the SI along with electrostatic potential (ESP) maps (Figs S6 and S7, and secs. S4.1 and S4.2, respectively). The structure of the S$_0$ state is as expected, with the double CH−O hydrogen bonds of the OMe groups on DMSP being apparent. The S$_1$ state is clearly different with the two OMe groups moving into the plane of the DMSP ligand. The ESP confirms a charge transfer state, with more positive charge on the methoxy groups and a more negatively charged nitrogen atom compared to the S$_0$ state. The S$_0$-S$_1$ adsorption (336.9 nm) and emission (456.4 nm) correlate well to experiment.

The optimized structures for the S$_0$ ground state of 1^{2+} and 2^{2+} (from two different viewpoints) are also given in the SI (Secs. S4.3 and S4.4). It should be noted that there are different possible conformers for 1^{2+}, which differ through a rotation of the OMe

group in the meta position. However, it was found that our conclusions are insensitive of the precise conformer chosen. Therefore, the focus here is on that conformer for which most excited state information was obtained in the calculations. Please see the ESI (Section S1.1.) for further discussion of this point.

The rotation barrier about the centre of the DMSP ligand in 1^{2+} is calculated as $\Delta G = 28.2$ kJ mol^{-1} and $\Delta H = 25.6$ kJ mol^{-1} at 298K, indicating that the structure is relative rigid and likely fairly reflects the solution structure. Given their structural similarities, the corresponding barrier for the same processes in 2^{2+} should also be close to that obtained for 1^{2+}. The calculated absorption spectra of 1^{2+} and 2^{2+} show a good general agreement between theory and experiment – Fig 3, with the positioning of the three major transitions coming very close to the experimental data.
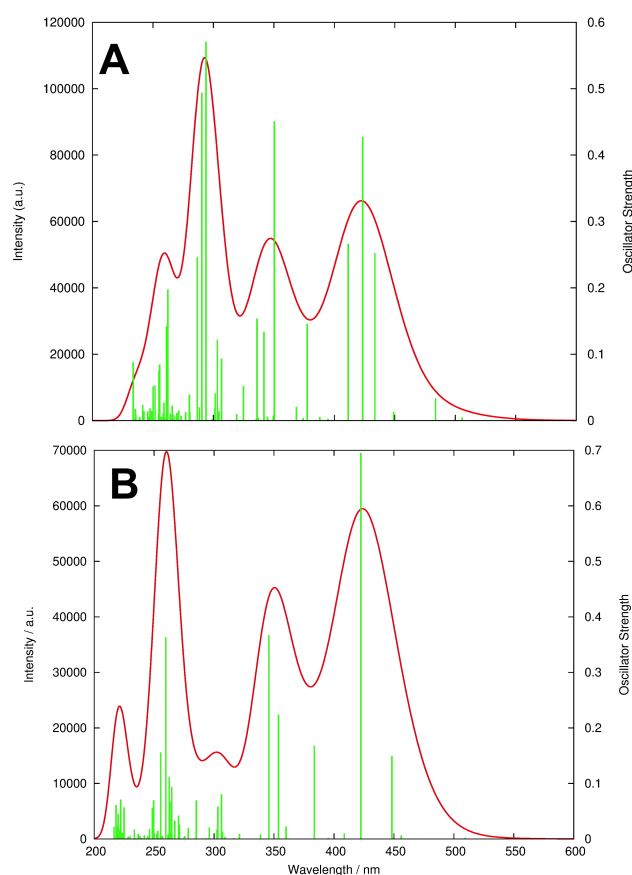

Fig. 3 Calculated transitions and spectra for **1** (A) and **2** (B).

Given the striking emission results, the lowest excited states of 1^{2+} and 2^{2+} were considered in detail – see Fig 4. Here, we noted that the lowest two singlet excitations of 1^{2+} are clearly charge transfer in character (see table S1 and Fig S9). First, the lowest triplet states of 1^{2+} and 2^{2+} were optimized. The structural changes for their T$_1$ states are relatively minor (see SI, Secs S4.5 and S4.6). If a pure 0-0 transition is assumed, emission from 1^{2+} occurs at 665 nm (and at 656 nm for 2^{2+}); if vibrational contributions are ignored, then emission at 637 nm and at 627 nm, respectively, is predicted. Both methods yield a triplet emission close to experimentally observed wavelengths, confirming the assignment of these bands.

The mapped electrostatic potential of complex 1^{2+} (Figure 4b) shows that this state is a charge transfer, with the donor being the tpmRu unit. A related analysis involving 2^{2+} produces a similar result.

The situation is more complicated for the emission at 540 nm; this could be emission from a lower-lying singlet or triplet states. However, given that – even for 1^{2+} - this emission occurs in water, it must be based on DMSP and not dppz. Since it has been suggested that the DMSP ligand can isomerize from its *trans* to *cis* form resulting a red shift in emission,[46] the possibility that this could occur for the coordinated ligand was also investigated; but an analysis for this putative process revealed that the calculated energies are totally inconsistent with the observed emission energies (see SI, Sec S4.7). Therefore, emission from other excited triplet states were considered.
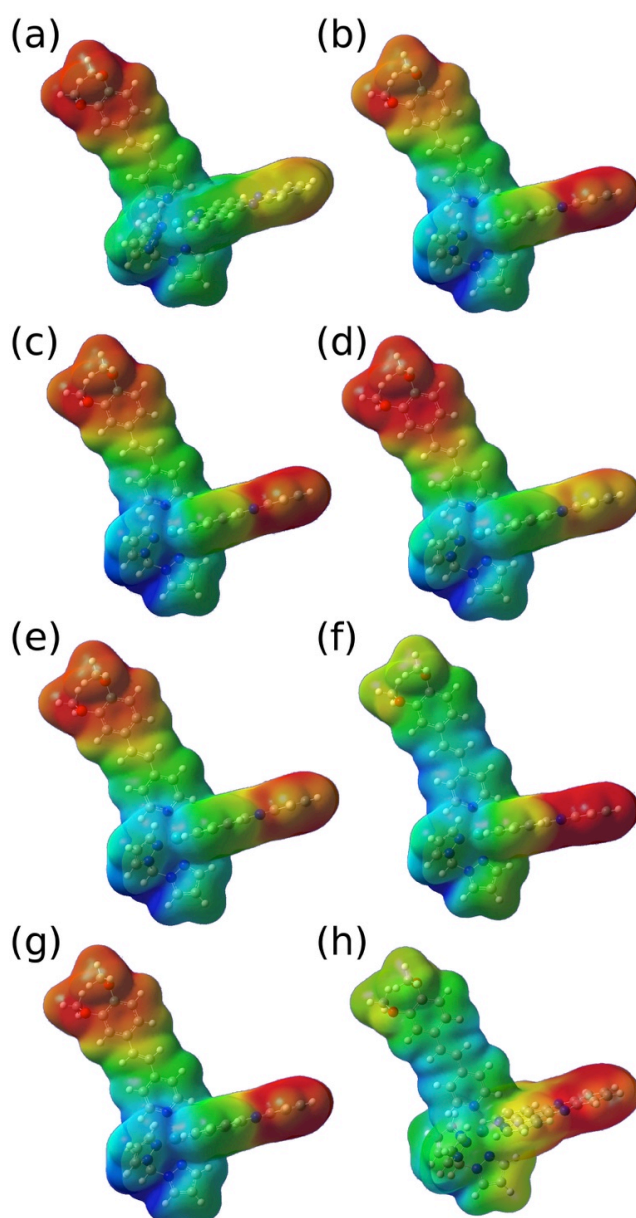

Fig. 4 Electrostatic potential of 1^{2+} in 8 different electronic states. All geometries are optimized for the specific electronic state except where indicated otherwise. Panel (a): S$_0$; Panel (b): T$_1$; Panel (c): T$_2$; Panel (d):

S5 (S0 geometry); Panel (e): S6 (S0 geometry); Panel (f): S7 (S0 geometry); Panel (g): S8 (S0 geometry); Panel (h): S2. It should be noted that, because the overall charge on the molecule is 2+, the scale has been shifted so that red corresponds to a charge of 0.075e and blue to a charge of +0.25e.

There are many close-lying triplet states above T_1 and their nature is highly dependant on their exact geometry (see the SI, Fig S12, for triplet states in various geometries,). Thus, an attempt was made to optimize these excited triplet states; an approach that proved successful for T_2 - see Fig 4(c) for the resulting ESP. This state has significantly more charge on the DMSP ligand and is closer to the S_0 state in this regard. In-line with the experimental data, emission from the T_2 state to the S_0 state (ignoring vibrational contributions) is predicted to occur at 543.1 nm. Optimization of higher triplet states was unsuccessful due to root crossing, but the possibility that one of these states is an even better candidate for the emission at 540 nm cannot be discounted.

The reason why two triplet states are emissive is due to an absorption process in which several singlet states are occupied. In our TD-DFT calculations on the singlet manifold using the S_0 geometry, there are three transitions with large oscillator strengths at energies employed in the experimental studies: S_0-S_5 at 433.5 nm, S_0-S_6 at 423.4 nm, and S_0-S_8 at 411.3 nm; S_6 is near-degenerate with S_7, which only has a small oscillator strength for transitions from the ground state (see table S1). From the ESPs plotted in Figure 4(d)-4(g) for the S_5-S_8 states, respectively, it is clear the nature of these states is very different. Whereas S_6 has significant charge transfer onto the dppz ligand, this is not the case for S_5, which largely shows charge transfer onto DMSP.

Even though this latter transition is fully consistent with the optical properties of 1^{2+} other possibilities for the high-energy emissive state were also explored, but none proved to be suitable candidates. For example, the possibility that emission at 540 nm is from a singlet state was also explored and an optimized structure for the S_1 and S_2 states was obtained (see SI – Secs S4.10 and S4.11). If solely singlet states are involved, it is most likely that emission would be due to an S_2 to S_0 transition, which is calculated to occur at 528.8 nm. However, the ESP [Fig. 4(h)] clearly shows that S_2 is formed by CT from tpmRu to dppz. This would lead to emission quenching by water, which is not observed experimentally, *vide infra*. In summary, these calculations indicate that the emission seen at 540 nm for 1^{2+} is from the T_2 to S_0 transition, and that T_1 and T_2 are both populated due to simultaneous excitation of singlet states of very different character.

Further support for this hypothesis comes from a closer study of the complex's luminescence properties in MeCN. Although excitation into the main ^{1}MLCT absorption band of 1^{2+} results in the dual emission described above, excitation at longer wavelengths (~500 nm) solely produces emission from the lower emission manifold centred at 680 nm, indicating that only the lower energy MLCT state is populated at this lower excitation energy

The complexes were converted into water soluble chloride salts through counterion metathesis and their optical properties in water were then explored. Whilst the emission of 2^{2+} in aqueous buffer shows very little difference to that in acetonitrile, this is not true for complex **1**. The low energy emission of 1^{2+} is from a Ru[II]→dppz-based ^{3}MLCT state and it is well-established that - due to enhanced hydrogen-bonding interactions - this excited state is quenched in protic solvents;[1] thus it might be expected that this emission may be affected by a change of solvent. Indeed, the emission of 1^{2+} in water *is* strikingly different, as excitation at 430 nm leads *only* to the emission at 550 nm – see SI Fig S13. The DNA binding properties of both complexes were then investigated.

DNA intercalators lengthen duplexes on binding, increasing the relative viscosity of aqueous DNA solutions, whereas typical groove-binding molecules induce no such change.[53,54] Given that 1^{2+} incorporates the known intercalative moiety dppz, whilst both complexes contain the putative groove binding ligand DMSP, we investigated any change of viscosity in calf thymus DNA, CT-DNA, induced by the complexes compared to the minor groove binder Hoechst 33258 (H33258) and the confirmed duplex intercalator, [Ru(tpm)(py)(dppz)]$^{2+}$.

This experiment showed that addition of 1^{2+} produces increases in viscosity that are comparable to [Ru(tpm)(dppz)(py)]$^{2+}$. In contrast, addition of 2^{2+} results in a significant *decrease* in viscosity - Fig 5. This response is often observed with metal complex groove binders as steric demand within a groove causes DNA bending leading to a reduction in hydrodynamic length of the duplex. [38,53-55] Since these results indicate that both complexes do interact with duplex DNA, the effect of CT-DNA on their emission properties was investigated.
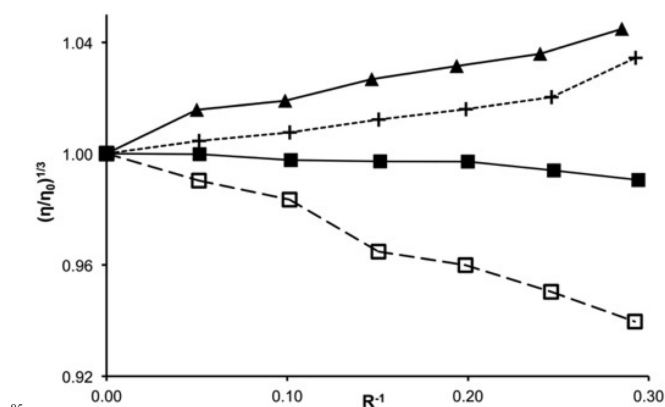

Fig. 5 Plots of relative viscosity changes induced by the addition of [**1**]Cl2 (+) and [**2**]Cl2 (□) compared to the effects of the confirmed intercalator [Ru(tpm)(dppz)(py)]Cl2 (▲),and the groove binder H33258 (■) in the same conditions. The connecting lines do not imply a fit to a model but are included to aid visualization of these data. Conditions: 5 mM Tris, 25 mM NaCl, pH 7.4 at 27 °C

For both complexes absorption titrations lead to spectral changes typically observed in interactions with DNA, with MLCT bands showing appreciable hypochromism – see SI Figs S14 and S15.. McGhee-von Hippel model[56] fits to binding curves constructed from this data yields estimated binding parameters of 1.8 x 10^6 M^{-1} (s = 1.1) for 1^{2+} and 2.0 x 10^5 M^{-1} (s = 0.6) for 2^{2+}. Compared to our studies on related complexes containing extended ancillary ligands, the estimated K_b value for **1** is particularly high; for example, [Ru(tpm)(dppz)(dpp)]$^{2+}$ (where = dpp = 4,4′dipyridyl-1,5-pentane) binds to DNA over an order of magnitude more weakly than 1^{2+}.[35] This suggests that the potentially groove binding coordinated DMSP ligand could be enhancing the intercalative interaction of the Ru(dppz) unit.

Certainly, the data for non-intercalating complex 2^{2+} supports this hypothesis as its relatively high binding affinity is comparable to those reported for related Ru[II]-based groove binders.[38,57] The effects of DNA binding on the luminescent properties of the complexes provided more evidence to explore this hypothesis.

The two complexes display very different emission responses to DNA. Addition of CT-DNA to complex 2^{2+} results in pronounced enhancement in its high-energy emission until it becomes as intense as the [3]MLCT-based luminescence –Fig 6A. Contrastingly, although addition of CT-DNA to aqueous solutions of 1^{2+} has only a little effect on the high energy band, the Ru[II]→dppz-based transition shows growth of an emission band at 660 nm typical of an DNA light switch effect –Fig 6B. The final emission profile of 1^{2+} on addition of excess CT-DNA is very similar to that in MeCN – SI Figs S17 and S18.
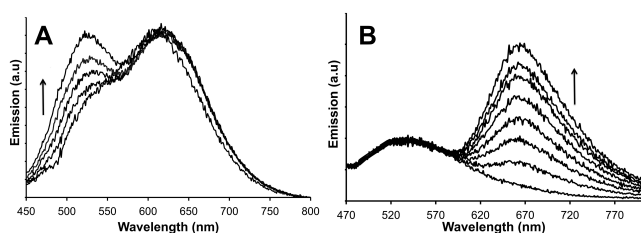

Fig. 6 (A) Luminescence changes in an aqueous buffer solution of [**2**]Cl$_2$ on initial additions of CT-DNA. (B) Luminescence changes in an aqueous buffer solution of [**1**]Cl$_2$ on initial additions of CT-DNA Conditions: 5 mM Tris, 25 mM NaCl, pH 7.4 at 25°C.

The DNA induced changes in the emission of complex 2^{2+} are consistent with our previous reports on related groove binders and confirm that complex 2^{2+} is interacting through such an interaction. However, contrastingly, it is noticeable that while the MLCT band of complex 1^{2+} displays the expected light-switch response, the higher energy transition is unaffected. Taken with the viscosity experiments, these observations suggest that although 1^{2+} is a confirmed intercalator the DMSP ligand does not sit deep enough to create true groove binding interactions. Certainly, in related systems, we have found that whether groove binding and/or intercalation occurs is highly dependent to the nature and connectivity of individual ligands coordinated to the tpmRu[II] unit.[37,38]

Although the changes in emission for complex 2^{2+} could not be successfully fitted to the McGhee-von Hippel model, fits for 1^{2+} yielded binding parameter estimates - 3.2 x 10^6 M^{-1} (s = 2.0) that are in good agreement to those from absorption titrations, again indicating high affinity binding.

The effect of CT-DNA addition to solutions of [**1**]Cl$_2$ is also easily visualized by the naked eye, being seen as a green-to-orange emission change – Fig 7A. More interestingly still, the very large changes in the (660 nm/540 nm) ratio of emission bands leads to a linear calibration plot for DNA concentrations from nanomolar concentrations up to ~30 μmol/bp – Fig 7B. Above this value the response is non-linear as binding saturation is approached.
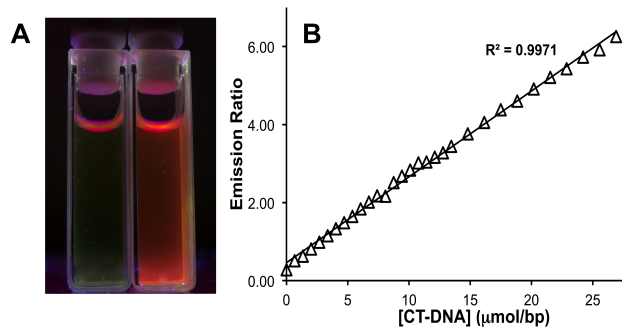

Fig. 7 (A) Naked eye detectable change in luminescence before (left) and after (after) addition of CT-DNA. (B) Calibration curve for [DNA] based on the changes in the (660 nm/540 nm) ratio of emission bands. The continuous line is a linear fit to these data. Conditions: 5 mM Tris, 25 mM NaCl, pH 7.4 at 25°C.

Conclusions

In conclusion, the studies reported herein illustrate how both the biophysical and photophysical characteristics of light-switch complexes can be modulated through judicious selection of ancillary ligands, leading to systems with entirely new properties. This approach has led to the synthesis of the first DNA light switch system to bind duplex DNA through a combination of groove binding and intercalation. As this complex displays dual emission properties and one of the emissive states is sensitive to DNA binding, uniquely, it is also a ratiometric probe for DNA.

Since, we have already demonstrated that the binding selectivities of Ru[II] complexes can be tuned to different cellular targets,[28,58-60] this suggests that further applications - as selective biosensors and bioprobes within cells - are a distinct possibility. More detailed studies on related derivatives aimed at targeting such functions and fully deconvoluting the contribution of each binding-mode are currently underway.

Notes and references

[a] Department of Chemistry University of Sheffield, Sheffield, S3 7HF, UK; Fax: (+) 44 114 222 934;. E-mail: a.meijer@sheffield.ac.uk, james.thomas@sheffield.ac.uk,,
[b] CSIR-National Chemical Laboratory, Pune: 411008, Maharashtra, India
[b] Dr. Amitava Das, CSIR-Central Salt & Marine Chemicals Research Institute. Bhavnagar, 364002, Gujarat (India). Fax: (+91) 2782567562; E-mail a.das@csmcri.res.in
† Electronic Supplementary Information (ESI) available: [details of any supplementary information available should be included here]. See DOI: 10.1039/b000000x/

1   A. E. Friedman, J. C. Chambron, J. P. Sauvage, N. J. Turro and J. K. Barton, *J. Am. Chem. Soc.*, 1990, **112**, 4960–4962.
2   K. E. Erkkila, D. T. Odom and J. K. Barton, *Chem. Rev.*, 1999, **99**, 2777–2796.

3   B. M. Zeglis, V. C. Pierre and J. K. Barton, *Chem. Commun.*, 2007, 4565–4579.

4   K. K.-W. Lo, M.-W. Louie and K. Y. Zhang, *Coord. Chem. Rev.*, 2010, **254**, 2603–2622.

5   A. W. McKinley, P. Lincoln and E. M. Tuite, *Coord. Chem. Rev.*, 2011, **255**, 2676–2692.

6   M. R. Gill and J. A. Thomas, *Chem Soc Rev*, 2012, **41**, 3179–3192.

7   A. C. Komor and J. K. Barton, *Chem. Commun.*, 2013, **49**, 3617–3630.

8   A. J. McConnell, H. Song and J. K. Barton, *Inorg Chem*, 2013, **52**, 10131–10136.

9   A. N. Boynton, L. Marcélis and J. K. Barton, *J. Am. Chem. Soc.*, 2016, **138**, 5020–5023.

10   N. P. Cook, V. Torres, D. Jain and A. A. Martí, *J. Am. Chem. Soc.*, 2011, **133**, 11121–11123.

11   N. P. Cook, K. Kilpatrick, L. Segatori and A. A. Martí, *J. Am. Chem. Soc.*, 2012, **134**, 20776–20782.

12   N. P. Cook, M. Ozbil, C. Katsampes, R. Prabhakar and A. A. Martí, *J. Am. Chem. Soc.*, 2013, **135**, 10810–10816.

13   A. Aliyan, B. Kirby, C. Pennington and A. A. Martí, *J. Am. Chem. Soc.*, 2016, **138**, 8686–8689.

14   R. Y. Tsien and M. Poenie, *Trends Biochem Sci*, 1986, **11**, 450–455.

15   Z. Liu, W. He and Z. Guo, *Chem Soc Rev*, 2013, **42**, 1568–33.

16   M. H. Lee, J. S. Kim and J. L. Sessler, *Chem Soc Rev*, 2015, **44**, 4185–4191.

17   J. A. Thomas, *Chem Soc Rev*, 2015, **44**, 4494–4500.

18   A. Ojida, H. Nonaka, Y. Miyahara, S.-I. Tamaru, K. Sada and I. Hamachi, *Angew. Chem. Int. Ed.*, 2006, **45**, 5518–5521.

19   Y. Kurishita, T. Kohira, A. Ojida and I. Hamachi, *J. Am. Chem. Soc.*, 2010, **132**, 13290–13299.

20   L. Zhou, X. Zhang, Q. Wang, Y. Lv, G. Mao, A. Luo, Y. Wu, Y. Wu, J. Zhang and W. Tan, *J. Am. Chem. Soc.*, 2014, **136**, 9838–9841.

21   T. Yoshihara, Y. Yamaguchi, M. Hosaka, T. Takeuchi and S. Tobita, *Angew. Chem. Int. Ed.*, 2012, **51**, 4148–4151.

22   T. J. Sørensen, A. M. Kenwright and S. Faulkner, *Chem. Sci.*, 2015, **6**, 2054–2059.

23   J. Paul, S. Spey, H. Adams and J. A. Thomas, *Inorg. Chem. Commun.*, 2004, **357**, 2827–2832.

24   C. Metcalfe, M. Webb and J. A. Thomas, *Chem. Commun.*, 2002, 2026–2027.

25   C. Metcalfe, C. Rajput and J. A. Thomas, *J. Inorg. Biochem.*, 2006, **100**, 1314–1319.

26   T. Phillips, C. Rajput, L. Twyman, I. Haq and J. A. Thomas, *Chem. Commun.*, 2005, 4327–4329.

27   C. Rajput, R. Rutkaite, L. Swanson, I. Haq and J. A. Thomas, *Chem. Eur. J.*, 2006, **12**, 4611–4619.

28   M. R. Gill, J. Garcia-Lara, S. J. Foster, C. Smythe, G. Battaglia and J. A. Thomas, *Nat Chem*, 2009, **1**, 662–667.

29   M. R. Gill, H. Derrat, C. G. W. Smythe, G. Battaglia and J. A. Thomas, *Chembiochem*, 2011, **12**, 877–880.

30   H. Ahmad, A. Wragg, W. Cullen, C. Wombwell, A. J. H. M. Meijer and J. A. Thomas, *Chem. Eur. J.*, 2014, **20**, 3089–3096.

31   C. Metcalfe, H. Adams, I. Haq and J. A. Thomas, *Chem. Commun.*, 2003, 1152–1153.

32   P. Waywell, V. Gonzalez, M. R. Gill, H. Adams, A. J. H. M. Meijer, M. P. Williamson and J. A. Thomas, *Chem. Eur. J.*, 2010, **16**, 2407–2417.

33   M. G. Walker, V. Gonzalez, E. Chekmeneva and J. A. Thomas, *Angew. Chem. Int. Ed. Engl.*, 2012, **51**, 12107–12110.

34   S. P. Foxon, C. Metcalfe, H. Adams, M. Webb and J. A. Thomas, *Inorg Chem*, 2007, **46**, 409–416.

35   C. Metcalfe, I. Haq and J. A. Thomas, *Inorg Chem*, 2004, **43**, 317–323.

36   S. P. Foxon, T. Phillips, M. R. Gill, M. Towrie, A. W. Parker, M. Webb and J. A. Thomas, *Angew. Chem. Int. Ed. Engl.*, 2007, **46**, 3686–3688.

37   H. Saeed, I. Saeed, N. Buurma and J. A. Thomas, *Chem. Eur. J.*, 2017, **23**.

38   A. Ghosh, P. Das, M. R. Gill, P. Kar, M. G. Walker, J. A. Thomas and A. Das, *Chem. Eur. J.*, 2011, **17**, 2089–2098.

39   R. L. Blakley, M. L. Myrick and M. K. DeArmond, *J. Am. Chem. Soc.*, 1986, **108**, 7843–7844.

40   A. P. Wilde, K. A. King and R. J. Watts, *J. Phys. Chem.*, 1991, **95**, 629–634.

41   T. E. Keyes, C. M. O'Connor, U. O'Dwyer, C. G. Coates, P. Callaghan, J. J. McGarvey and J. G. Vos, *J. Phys. Chem. A*, 1999, **103**, 8915–8920.

42   L.-Q. Song, J. Feng, X.-S. Wang, J.-H. Yu, Y.-J. Hou, P.-H. Xie, B.-W. Zhang, J.-F. Xiang, X.-C. Ai and J.-P. Zhang, *Inorg Chem*, 2003, **42**, 3393–3395.

43   E. C. Glazer, D. Magde and Y. Tor, *J. Am. Chem. Soc.*, 2005, **127**, 4190–4192.

44   R. Siebert, A. Winter, U. S. Schubert, B. Dietzek and J. Popp, *Phys. Chem. Chem. Phys.*, 2011, **13**, 1606–1617.

45   C. Kreitner, M. Grabolle, U. Resch-Genger and K. Heinze, *Inorg Chem*, 2014, **53**, 12947–12961.

46   A. J. Amoroso, A. Das, J. A. McCleverty, M. D. Ward, F. Barigelletti and L. Flamigni, *Inorg Chim Acta*, 1994, **226**, 171–177.

47   A. Ryabchun, A. Bobrovsky, V. Shibaev, S. Gromov, N. Lobova and M. Alfimov, *J Photochem Photobiol A*, 2011, **221**, 22–29.

48   M. K. DeArmond and C. M. Carlin, *Coord Chem Rev*, 1981, **36**, 325–355.

49   X.-Y. Wang, A. Del Guerzo and R. H. Schmehl, *J. Photochem. Photobiol. C: Photochem. Rev.*, 2004, **5**, 55–77.

50   K. K.-W. Lo, K. Y. Zhang, S.-K. Leung and M.-C. Tang, *Angew. Chem. Int. Ed.*, 2008, **47**, 2213–2216.

51   S. Sharma, H. Kim, Y. H. Lee, T. Kim, Y. S. Lee and M. H. Lee, *Inorg Chem*, 2014, **53**, 8672–8680.

52   D. Magde, M. D. Magde Jr and E. C. Glazer, *Coord Chem Rev*, 2016, **306**, 447–467.

53   S. Satyanarayana, J. C. Dabrowiak and J. B. Chaires, *Biochemistry*, 1992, **31**, 9319–9324.

54   S. Satyanarayana, J. C. Dabrowiak and J. B. Chaires, *Biochemistry*, 1993, **32**, 2573–2584.

55   D. Ghosh, H. Ahmad and J. A Thomas, *Chem. Commun.*, 2009, 2947–2949.

56   J. D. J. McGhee and P. H. P. von Hippel, *J. Mol. Biol.*, 1974, **86**, 469–489.

57   G. I. Pascu, A. C. G. Hotze, C. Sanchez-Cano, B. M. Kariuki and M. J. Hannon, *Angew. Chem. Int. Ed.*, 2007, **46**, 4374–4378.

58   M. R. Gill, D. Cecchin, M. G. Walker, R. S. Mulla, G. Battaglia, C. Smythe and J. A. Thomas, *Chem. Sci.*, 2013, **4**, 4512–4519.

59   A. Wragg, M. R. Gill, D. Turton, H. Adams, T. M. Roseveare, C. Smythe, X. Su and J. A. Thomas, *Chem. Eur. J.*, 2014, **20**, 14004–14011.

60   A. Wragg, M. R. Gill, L. McKenzie, C. Glover, R. Mowll, J. A. Weinstein, X. Su, C. Smythe and J. A. Thomas, *Chem. Eur. J.*, 2015, **21**, 11865–11871.